ISBN: 978-3-95450-184-7 doi:10.18429/JACoW-IPAC2018-TUYGBF4

DESIGN AND SIMULATION TOOLS FOR THE HIGH-INTENSITY INDUSTRIAL RHODOTRON ELECTRON ACCELERATOR

W. Kleeven*, M. Abs, J. Brison, E. Forton, J. Van de Walle, J.-M. Hubert
IBA, Chemin du Cyclotron 3, B-1348 Louvain-la-Neuve, Belgium

Abstract

The Rhodotron is a compact industrial CW recirculating electron accelerator producing intense beams with energies in the range from about 1 to 10 MeV. RF-frequencies are in the range of 100 to 400 MHz. Average beam powers can range from 10 kW to almost 1 MW, depending of the specific type of Rhodotron. Main industrial applications are polymer cross-linking, sterilization, food treatment and container security scanning. Recently, RF pulsing was developed to reduce the average wall power dissipation, thus reducing drastically the energy consumption. Pulsing also permits smaller cavities and higher energies up to 40 MeV, opening the way to applications such as mobile irradiators, or isotopes production by photonuclear reactions, thus offering a compact and high beam duty alternative to linacs. This paper concentrates on some crucial design tools and methods for transverse and longitudinal optics studies, particle tracking with space charge, beam formation studies in the electron gun and dipole magnet design.

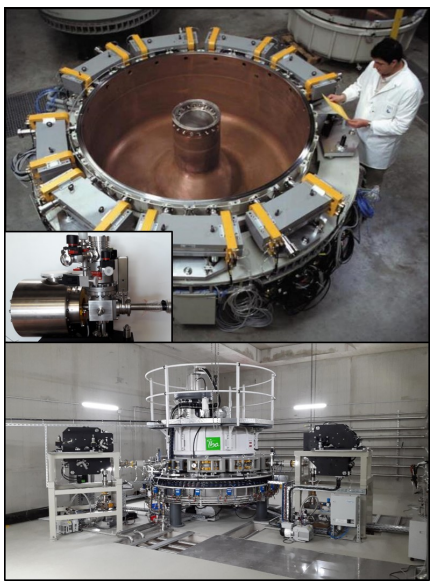

Figure 1: A rhodotron is shown, with dipoles arranged around the coaxial RF cavity, the egun (small inset) and the full system with two external beam lines.

PRINCIPLE AND APPLICATIONS

The rhodotron has been described in multiple publications [1–4]. Beam is injected radially from the egun into the coaxial RF-cavity (Fig. 1) and is accelerated a first time when passing from the outer cavity wall towards the cavity inner pillar. During the pillar transit, the electric field changes sign and the beam is accelerated again when passing from the pillar back towards the outer wall. After the first pass exit, a dipole magnet re-injects the beam into the cavity (see also Fig. 8). In this outside transit, the electric field again changes sign allowing acceleration in a 2nd pass through the cavity. This pattern is repated several (order 10) times. Main applications are illustrated in Fig. 2.

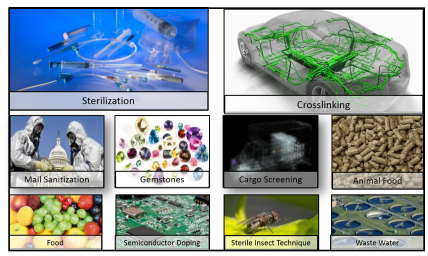

Figure 2: Examples of Rhodotron accelerator applications.

SIMULATION TOOLS AND METHODS

A Simple Model for the Transverse Optics

This model (Fig. 3) calculates linear optics along one period (optical cell) of the turn-pattern. The half-period consists of a drift l, a pole face rotation (angle β) and a uniform bend (angle $\pi + 2\gamma$). The pole face optics depends on the fringe field integral k_1 (Ref. [5]). The betatron phase advance per cell [6] Φ is obtained from the trace of the full period transfer matrix M as $\cos\Phi = \frac{1}{2}\mathrm{Trace}(M)$. The upper of Fig. 4 shows Φ_x and Φ_z as a function of β. Best stability is obtained for $\Phi_x \approx \Phi_z$ and small values of k_1. Dipole field clamps are used to obtain this condition. The lower of Fig. 4 shows the optimization of the beta-functions that can be achieved by proper choice of β.

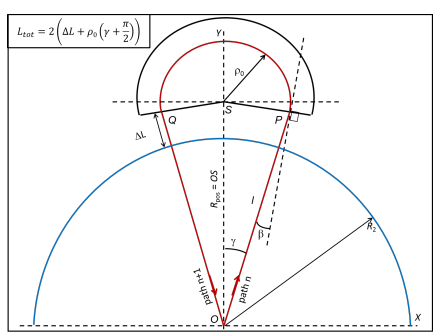

Figure 3: Geometry of one period of acceleration.

* willem.kleeven@iba-group.com

ISBN: 978-3-95450-184-7 doi:10.18429/JACoW-IPAC2018-TUYGBF4

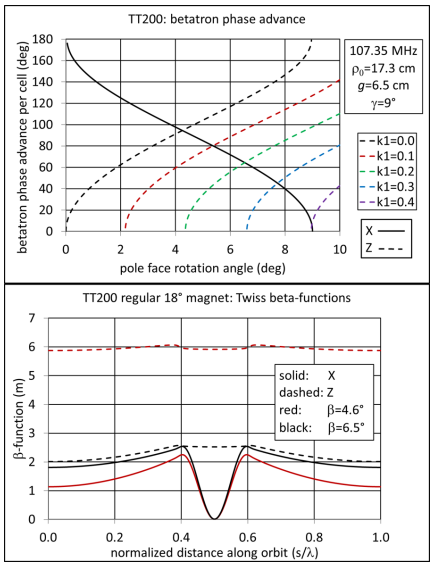

Figure 4: Betatron phase advances along one cell, and beta-functions calculated with the tracking code AOC [7].

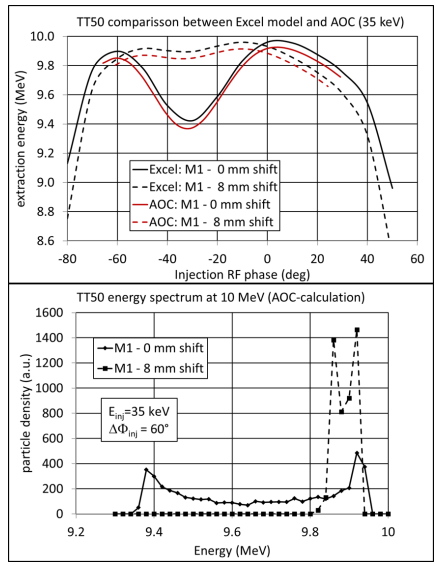

Figure 5: Dependence of extraction energy on the injected RF phase and illustration of the improvement of the energy spread by proper positioning of dipole M1.

A Simple Model for the Longitudinal Optics

The cavity oscillates in an almost perfect TEM mode with a radial electric field component equal to $E_r(r) = V_0/(r\ln(R_2/R_1))$, ($V_0$ =cavity voltage; R_1 and R_2 =inner and outer coax radii). The equations of motion have been implemented in an Excel model that tracks subsequent passes through the cavity. In a first step the model calculates a particle that gains maximum energy. This is achieved by optimizing (with the Excel solver), the injection phase of the first pass and subsequently, the orbit length through each dipole (Fig. 3) of all subsequent passes. This procedure gives "optimum" positions and field values (or PSU-settings) of all dipoles. In a second step, it is allowed to shift dipoles away from the initial positions. PSU-settings are then accordingly adopted. In a third step, a range of (non-ideal) injection phases are calculated. Figure 5 shows the dependance of extraction energy on the injection phase and compares with the in-house full 3D tracking code AOC [7]. The simple model shows that a much better energy resolution is obtained by shifting the first dipole M1 away from the "ideal" position. This result is confirmed by AOC (lower of Fig. 5).

RF Cavity Field Computations for Tracking

Since the cavity RF mode is almost perfectly TEM, the fields near the median plane can be obtained with an electrostatic 3D finite element solver like Opera3D [8]. Figure 6 shows a cavity geometrie that has been solved in this way. Comparing with full 3D RF solvers, this allows (in general), to use more detailed meshing in critical zones such as the beam holes in the cavity wall and inner pillar, where transverse electrical focusing can be strong. We use this method to generate full 3D maps for tracking in AOC. The lower left of Fig. 6 shows as an example the radial electric field along the injection axis. The azimuthal component B_θ of the RF magnetic field close to the median plane is also obtained (and used in AOC), since it is related to the median plane electric field E_{r0} as: $E_r = E_{r0}\sin\omega t$, $B_\theta = \frac{E_{r0}}{\eta_0}\tan(\omega z/c)\cos\omega t$, where η_0 is the vacuum impedance.

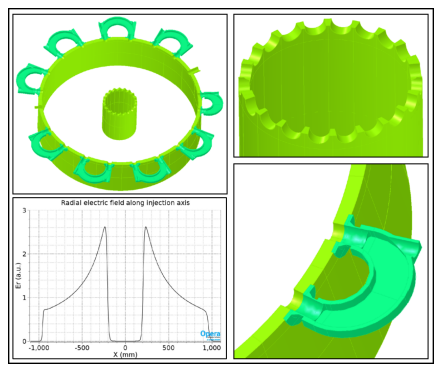

Figure 6: Modeling of the TT300 RF cavity in Tosca.

3D Magnetic Field Computations

Opera3D [8] is used to generate full 3D field maps of the dipole magnets. Multiple maps can be imported in AOC [7]. Also the two egun solenoids are usually included. AOC allows to position and orient each map with 5 degrees of freedom. Maps can be linearly scaled to simulate adjustment of PSU-values. A same map can be used more than once, in order to include a same magnet placed at multiple positions. In regions where maps overlap, the user can choose to only take into account the field of the most relevant map, or to accumulate the fields of multiple magnets. In this way, the full rhodotron magnetic structure can be constructed and tuned, for optimum beam transmission from injection to extraction. Low energy electrons are extremely sensitive to stray and earth magnetic fields. We take these into account by constructing an Opera3D model of all magnets together that also

ISBN: 978-3-95450-184-7 doi:10.18429/JACoW-IPAC2018-TUYGBF4

includes other subsytems made of magnetic iron. Figure 7 shows an example of the TT40MeV which is currently under study. This machine will be used for isotope production by photo-nuclear reactions. It will be pulsed to reduce average wall power and thus obtain the required high energies. Not only the support structure of the magnets and of the rhodotron is included but also an egun shielding plate and the cavity itself. This cavity is made of (magnetic) iron and copper plated on the inside. Around the outer cavity, a pair of large solenoids is placed. They allow to globally fine tune the beam position especially during the first pass where the energy is low. This solenoid field map is separately included in the tracking simulations. The inset in Fig. 7 shows the cross-talk field map. This is the difference between the field map of the full structure (including the support structures, the cavity and also the interaction between magnets) and the sum of all independent magnets. This cross-talk map is also included in the tracking.

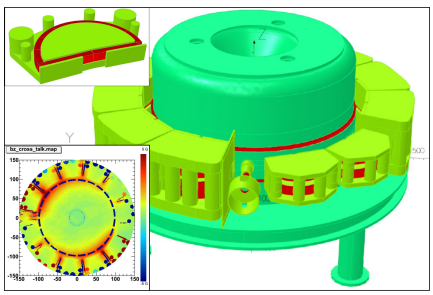

Figure 7: Full Opera3D magnetic model of the TT40MeV.

Full 3D Particle Tracking with Space Charge

AOC tracking may include the full 3D electric and magnetic self-fields, calculated for a bunch in free space. These effects are important, especially within the egun and during the first pass where the electron energies are not yet high. Figure 8 shows such a beam in the very compact TT50. This 10 MeV pulsed industrial rhodotron has been recently developed for cargo screening. The dipoles are permanent magnet dipoles (except the first one). The self-consistent space charge beam with an average current of 10 mA (roughly 100 mA peak in the bunch) is calculated from the 35 kV electron gun up to extraction. The inset in Fig. 8 shows the radial positions and the magnetic field setpoints of the dipoles as obtained from the simple longitudinal model. These values are always very close to the final settings obtained from the AOC tracking.

Egun Simulation

Beam formation in the egun is simulated in a rotational symmetric model that is solved with the Opera2D [8] SP module. It contains (Fig. 9) a cathode-holder with cathode at high negative voltage, a beam extraction electrode (at ground), a bias electrode (preventing back-bombardment of the cathode by ionized rest-gas), a focusing solenoid and an iron shield (screening the beam path from magnetic stray

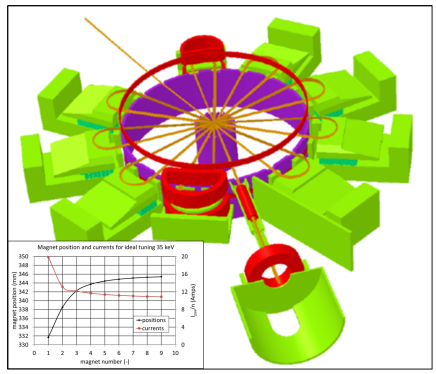

Figure 8: Full space charge simulated beam in the TT50.

fields). The model is solved first in magnetic mode, giving the solenoid field map; this map is then included in a second step of solving the self-consistent electric space charge. The cathode is treated as a Child-Langmuir emitter. Above its surface (at a distance of 50 to 100 µm), is a wire grid. The voltage difference between grid and cathode determines the extracted beam current. The grid is modeled as a series of circular concentric wires. In reality this geometry may be more complex but the simple model already matches rather good with operational experience. Figure 9 also shows zooms into the extraction geometry and shows details of the grid. The SP-sover calculates self-consistent beamlets (also shown in Fig. 9), that leave the cathode and pass through the grid. The model is solved for a number of different cathode-grid voltages; this allows to construct the realistic 6D phase space of a RF bunch needed for rhodotron tracking simulations.

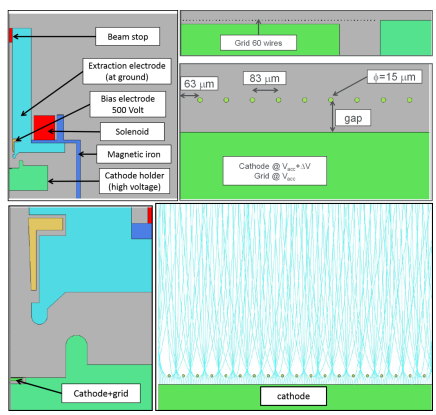

Figure 9: Illustration of the Opera2D egun-model.

RESULTS AND OUTLOOK

The new tools and methods have been very succesfully used in the construction and commissioning of the TT50; the latest member of the Rhodotron family. Full required beam intensity (10 mA peak) has been obtained with excelent stability and performance. Also acceleration of 3.5 MeV per pass has been succesfully tested in the TT300 in pulsed mode; this prepares the road for the TT40MeV development.

ISBN: 978-3-95450-184-7 doi:10.18429/JACoW-IPAC2018-TUYGBF4

REFERENCES

[1] J. Pottier, "A new type of RF electron accelerator: the Rhodotron", Nucl. Instr. Meth. Phys. Res. vol. B40/41, pp. 943–945, 1989.

[2] J. M. Bassaler, J.M. Capdevilla, O. Gal, F. Laine, A. Nguyen, J.P. Nicolai, K. Umiastowski, "Rhodotron: an accelerator for industrial irradiation", Nucl. Instr. Meth. Phys. Res., vol. B68, pp. 92–95, 1992.

[3] Y. Jongen, M. Abs, T. Delvigne, A. Herer, J.M. Capdevila, F. Genin and A. Nguyen, "Rhodotron accelerators for industrial electron-beam processing : a progress report", Proc. 5th Eur. Part. Acc. Conf. (EPAC-96), Sitges-Barcelona, pp 2687-2689, 1996.

[4] M. R. Cleland, "Radio-Frequency Electron Accelerators for Industrial Applications", Rev. Acc. Sci. Techn., vol. 4, pp. 213-218, 2011.

[5] K.L. Brown, D.C. Carey, Ch. Iselin and F. Rothacker, "TRANSPORT: a computer program for designing charged particle beam transport systems", CERN report 80-04, March 1980.

[6] K. Steffen, "Basic Course on Accelerator Optics", Proc. Cern Acc. School (CAS) on Gen. Accel. Phys., Gif-sur-Yvette, France, September 1984. CERN report 85-19, November 1985, p. 25.

[7] W.J.G.M. Kleeven, M. Abs, E. Forton, V. Nuttens, E.E. Pearson, J. Van der Walle and S. Zaremba, "AOC, A Beam Dynamcis Code for Medical and Industrial Accelerators at IBA". Proc. 7th Int. Part. Acc. Conf. (IPAC), Busan, Korea, pp. 1902-1904, 2016.

[8] Cobham, http://http://operafea.com